A novel role in cytokinesis reveals a housekeeping function for the unfolded protein response

Alicia A. Bicknell, Anna Babour, Christine M. Federovitch, and Maho Niwa

Division of Biological Sciences, University of California, San Diego, La Jolla, CA 92093

The unfolded protein response (UPR) pathway helps cells cope with endoplasmic reticulum (ER) stress by activating genes that increase the ER's functional capabilities. We have identified a novel role for the UPR pathway in facilitating budding yeast cytokinesis. Although other cell cycle events are unaffected by conditions that disrupt ER function, cytokinesis is sensitive to these conditions. Moreover, efficient cytokinesis requires the UPR pathway even during unstressed growth conditions. UPR-deficient cells are defective in cytokinesis, and cytokinesis mutants activate the UPR. The UPR likely achieves its role in cytokinesis by sensing small changes in ER load and making according changes in ER capacity. We propose that cytokinesis is one of many cellular events that require a subtle increase in ER function and that the UPR pathway has a previously uncharacterized housekeeping role in maintaining ER plasticity during normal cell growth.

Introduction

The ER plays a crucial role in several important aspects of eukaryotic cell physiology. It assists in the folding and maturation of all nascent secretory proteins and initiates their distribution to the broader secretory pathway (Ellgaard et al., 1999). In addition, the ER influences the overall composition of the cellular proteome by mediating the ER-associated degradation (ERAD) pathway, a pathway that destroys misfolded proteins and also responds to specific degradation signals to regulate the levels of certain native proteins (Hampton, 2002). The ER also houses many lipid biosynthetic enzymes, which impact the relative composition and overall abundance of lipids throughout the cell (Daum et al., 1998).

Genes involved in protein folding, protein trafficking, ERAD, and lipid metabolism are all transcriptionally activated by a conserved ER-initiated signal transduction pathway called the unfolded protein response (UPR; Mori, 2000; Travers et al., 2000; Harding et al., 2001; Patil and Walter, 2001; Kaufman, 2002). In budding yeast, the UPR pathway begins with an ER transmembrane protein, Ire1p (Cox et al., 1993; Mori et al., 1993). The N terminus of Ire1p lies in the lumen of the ER, where it senses the ER's condition. When Ire1p detects a need for increased ER function, it transmits a signal across the ER membrane to activate its own cytosolic kinase and endoribonuclease domains (Cox et al., 1993; Mori et al., 1993; Shamu and Walter, 1996; Sidrauski and Walter, 1997). Activated Ire1p then initiates the unconventional splicesome-independent splicing of *HAC1* mRNA (Cox and Walter, 1996; Sidrauski and Walter, 1997). Only the spliced form of *HAC1* mRNA can be translated, making the splicing step a critical point of regulation (Chapman et al., 1998; Ruegsegger et al., 2001). Upon translation, Hac1p localizes to the nucleus, where it acts as a transcription factor to up-regulate a wide array of UPR target genes (Cox and Walter, 1996; Kawahara et al., 1997), thus increasing the ER's capacity to serve its many functions (Travers et al., 2000).

Northern analysis, which measures the relative abundance of spliced *HAC1* mRNA in the cell, is currently the most commonly used method of detecting UPR activation (Cox and Walter, 1996). Using this technique, previous studies have detected UPR activation only during extreme conditions of ER stress. For example, *HAC1* mRNA splicing has been detected in cells treated with pharmacological agents that cause widespread protein misfolding (Cox and Walter, 1996; Kawahara et al., 1997) or in cells overexpressing mutant proteins that fold improperly (Spear and Ng, 2003). The inability to detect *HAC1* mRNA splicing during normal growth has led to the designation of the UPR pathway as a stress response pathway. However, it is likely that cellular demand for ER function is dynamic even during unstressed growth conditions. This evokes the intriguing possibility that in addition to responding to conditions of extreme stress, the UPR pathway manages the everyday challenges of fluctuating ER demand. This housekeeping function for the UPR has been previously unnoticed, perhaps because it induces a level of Ire1p activity that is too subtle to be detected by conventional *HAC1* Northern analysis.

Correspondence to Maho Niwa: niwa@ucsd.edu

Abbreviations used in this paper: ERAD, ER-associated degradation; Tm, tunicamycin; UPR, unfolded protein response.

The online version of this article contains supplemental material.

The Journal of Cell Biology, Vol. 177, No. 6, June 18, 2007 1017–1027
http://www.jcb.org/cgi/doi/10.1083/jcb.200702101

Supplemental Material can be found at:
http://www.jcb.org/cgi/content/full/jcb.200702101/DC1

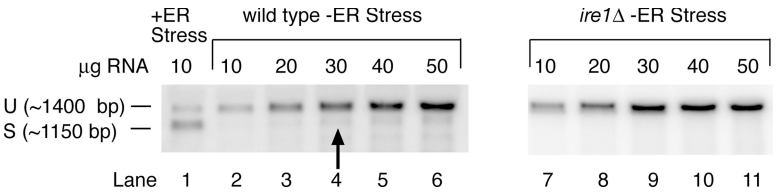

Figure 1. ***HAC1* mRNA splicing occurs during unstressed growth.** Wild-type cells (MNY1002) were treated with 1 μg/ml Tm for 1.5 h to induce UPR. 10 μg RNA were loaded on a Northern gel (lane 1). Indicated amounts of RNA from untreated asynchronous wild-type (MNY1002) cells (lanes 2–6) and *ire1Δ* (MNY1011) cells (lanes 7–11) were loaded on a Northern gel. The gel was probed with a *HAC1*-specific probe to detect unspliced (U) and spliced (S) forms. The arrow indicates the presence of spliced *HAC1* in the unstressed sample.

Because progression through the cell cycle requires dramatic molecular and cellular changes, we hypothesized that cell cycle progression requires fluctuations in ER capacity. To isolate a cell cycle event that requires particularly high ER functionality, we used ER stress as a tool to disrupt ER function. We then asked whether any particular cell cycle event was sensitive to this reduction in ER capacity. Most cell cycle events that we examined did not require exceptionally high ER activity, as they occurred normally during ER stress. However, cells experiencing ER stress were specifically defective in cytokinesis, suggesting that elevated ER functionality is required for cells to carry out efficient cytokinesis.

Because cytokinesis required a greater ER capacity than other cell cycle events, we tested the possibility that the UPR plays a role in achieving an increased ER capacity during normal, unstressed cytokinesis. Indeed, we found that UPR-deficient cells were unable to carry out efficient cytokinesis even in the absence of external ER stress. This is the first time the UPR pathway has been shown to function in cells that are growing optimally, expressing no misfolded mutant proteins, exposed to no protein misfolding agents, and not differentiating into high volume secretory cells. Therefore, our study supports the concept of a UPR that continuously fine tunes the ER to accommodate everyday fluctuations in ER functional demand.

Results

HAC1 mRNA splicing occurs during unstressed growth

Because previous *HAC1* Northern analysis has not uncovered HAC1 mRNA splicing in unstressed cells (Cox and Walter, 1996), we performed *HAC1* Northern analysis with 30 μg RNA rather than the 10 μg RNA that is traditionally assayed. Under these conditions, we could clearly detect the spliced form of *HAC1* in unstressed optimally grown wild-type cells. This spliced form constituted 7.4 ± 0.6% of total *HAC1* mRNA (Fig. 1). Basal splicing was *IRE1* dependent, suggesting the presence of a bona fide UPR signal in unstressed cells. The results of our Northern analysis, which we confirmed by RT-PCR (Fig. S1, available at http://www.jcb.org/cgi/content/full/jcb.200702101/DC1), prompted us to seek a functional relevance for basal UPR induction.

ero1-1 cells are delayed in the cell cycle with high DNA content, large buds, and divided nuclei

To determine whether this low level of UPR activity has a role in cell cycle progression, we used the *ero1-1* temperature-sensitive allele to identify cell cycle stages that are sensitive to ER perturbations. In the yeast ER, the essential proteins Ero1p (ER oxidoreductin 1) and Pdi1p (protein disulfide isomerase 1) work together to catalyze oxidative protein folding (Pollard et al., 1998; Frand and Kaiser, 1999; Tu et al., 2000). For cells carrying the *ero1-1* temperature-sensitive allele, growth at the restrictive temperature rapidly induces ER stress (Frand and Kaiser, 1998).

In asynchronous cultures, the restrictive growth of *ero1-1* cells caused an accumulation of cells with a 2C or greater DNA content (Fig. S2, available at http://www.jcb.org/cgi/content/full/jcb.200702101/DC1). This suggests that ER stress delays cell cycle progression at a point subsequent to DNA replication. To specifically define this ER-sensitive stage of the cell cycle, we induced ER stress in α-factor synchronized *ero1-1* cells (Fig. 2 A). When grown at the restrictive temperature, synchronized *ero1-1* cells experienced severe ER stress, as measured by *HAC1* splicing (Fig. 2, B and C). Compared with wild-type cells, these ER-stressed cells proceeded normally through the initial stages of the cell cycle. By 30 min after the temperature shift, both cell types completed DNA replication, thus adopting a 90–95% 2C DNA content (Fig. 2, D and quantitated in E). After 1 h of growth at 37°C, wild-type cells began to divide and reenter G1 phase. In contrast, only a small percentage of *ero1-1* cells divided at 37°C. Instead, ER-stressed cells retained a 2C DNA content or began to acquire abnormally high amounts of DNA (Fig. 2 D).

Microscopic examination of synchronized wild-type and *ero1-1* cells revealed that ER-stressed cells were delayed with large buds and divided nuclei. After 30 min of 37°C growth, 90% of cells of each cell type had initiated bud formation (Fig. 2, F and H). After 45 min, both cell types remained budded, and, by this time, 60–70% of both cell populations had divided nuclei (Fig. 2 G). After 1 h, wild-type cells began to divide and become newly divided unbudded cells with a single nucleus. In contrast, *ero1-1* cells did not divide but remained budded with divided nuclei for the remainder of the time course (Fig. 2, F and G), suggesting that ER stress slows the cell cycle at a point after nuclear division, probably during late M phase or cytokinesis. In fact, many *ero1-1* cells began to adopt a multibudded morphology after 1.5 h of 37°C growth (Fig. 2 H). This multibudded morphology was never seen in wild-type cells. The appearance of extra buds coupled with the appearance of 3C/4C DNA peaks strongly suggests that *ero1-1* cells initiate a new round of the cell cycle despite a block or delay in the previous cell division.

Tunicamycin-treated cells are delayed in the cell cycle with high DNA content, large buds, and divided nuclei

To confirm that ER stress is specifically responsible for delaying the cell cycle in *ero1-1* cells, we examined the effects of another well-characterized ER stress inducer, tunicamycin (Tm), on cell

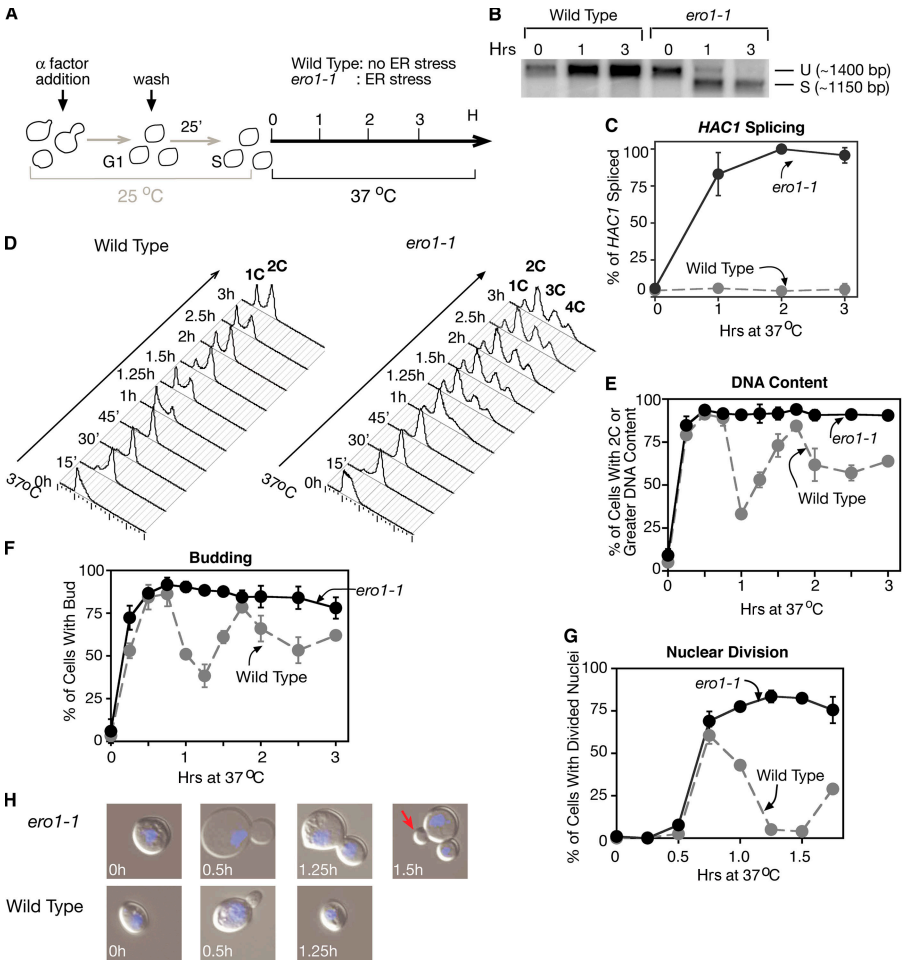

Figure 2. ***ero1-1* cells are delayed in the cell cycle with high DNA content, large buds, and divided nuclei.** Wild-type (MNY1002) and *ero1-1* (MNY1003) cells were shifted to 37°C after α-factor synchronization and 25 min of recovery at 25°C. The 25 min after α-factor removal prevented cells from undergoing the heat-specific G1/S phase delay that was observed in asynchronous experiments (Fig. S2, available at http://www.jcb.org/cgi/content/full/jcb.200702101/DC1), thus allowing the examination of subsequent ER-specific cell cycle effects. (A) Schematic representation of the experiment. Note that the 0-h time point is defined as the time of shifting to 37°C growth. (B) Northern analysis with a *HAC1*-specific probe shows the conversion of unspliced *HAC1* mRNA (U) to spliced *HAC1* mRNA (S) in *ero1-1* cells experiencing ER stress upon growth at 37°C. (C) Quantitation of B calculated as spliced *HAC1* mRNA divided by total *HAC1* mRNA. (D) Flow cytometric analysis of cells stained with Sytox green, a fluorescent dye that binds DNA quantitatively and emits fluorescence with an intensity corresponding to cellular DNA content (Haase and Reed, 2002). The first peak in the histogram (indicated as 1C) represents prereplication cells, and the second peak (2C) represents postreplication cells. The appearance of 3C and 4C cells is represented by a third and fourth peak. (E) Quantitation from D of the percentage of cells in the population that contained 2C or greater DNA content combined. (F) 200 cells per time point were scored as + or – bud. The graph represents the percentage of total cells that contained a bud. (G) Cells were stained with DAPI to visualize nuclei, and 200 cells per time point were scored as + or – divided nuclei. The graph represents the percentage of total cells that contained divided nuclei. (H) Cells were stained with DAPI. The red arrow indicates an additional bud. All error bars represent the SD of three repeats.

cycle progression. Tm inhibits N-linked glycosylation in the ER, which causes the accumulation of unfolded proteins. Consistent with previous studies (Arnold and Tanner, 1982; Vai et al., 1987), we found that Tm inhibits the budding process when added immediately after α-factor release (Fig. S3, available at http://www.jcb.org/cgi/content/full/jcb.200702101/DC1). Budding inhibition is known to activate the morphogenesis checkpoint and induce a G2/M delay (McMillan et al., 1998), which would likely obscure a subsequent ER-induced delay. Therefore, we introduced Tm to synchronized cultures 30 min after G1 release, after cells had already initiated the budding process (Fig. S3).

Tm treatment recapitulated the cell cycle effects of the *ero1-1* mutation. As expected, Tm-treated cells displayed 90% *HAC1* mRNA splicing 1 h after α-factor release (Fig. 3, A and B) and retained maximal UPR induction for the entire 3-h time course. Both Tm-treated and untreated synchronized cultures contained ∼90% 2C cells after 1 h, indicating that they had progressed through S phase and into G2/M phase (Fig. 3, C and D). After 1.25 h of growth , untreated cells began to divide, as indicated by the return to a 1C DNA content, and continued through the next cell cycle, ultimately losing synchronicity. Like *ero1-1* cells, Tm-treated cells failed to divide and instead began to attain a 3C or 4C DNA content (Fig. 3 C).

Untreated and Tm-treated cells were ∼90% budded after 1 h of synchronized growth (Fig. 3 E). After 1.5 h of growth, untreated cells divided and became unbudded before reentering the next cell cycle. Tm-treated cells remained 80–90% budded for the entire duration of the time course. Furthermore, after 1.75 h of growth, Tm-treated cells began to attain a multibudded morphology (Fig. 3 G).

We also examined the timing and integrity of nuclear division in Tm-treated cells. In addition to following the segregation of DAPI bodies in these cells, we expressed a GFP fusion protein that localized to both copies of chromosome IV (see Materials and methods). This allowed us to visualize sister chromatids segregating to separate nuclei during nuclear division (Biggins et al., 1999) to confirm that DNA segregation was occurring appropriately. We found that nuclear division occurred with the same kinetics in Tm-treated cells as in untreated cells, as both conditions allowed ∼45% of cells to divide their nuclei after 1 h of growth and ∼75% of cells to divide their nuclei after 1.25 h of growth (Fig. 3 F). After 1.5 h of growth, untreated cells divided to become unbudded cells with a single nucleus. Tm-treated cells continued to contain 70–80% divided nuclei for the remainder of the time course. Furthermore, we never observed DAPI bodies separating with improperly segregated

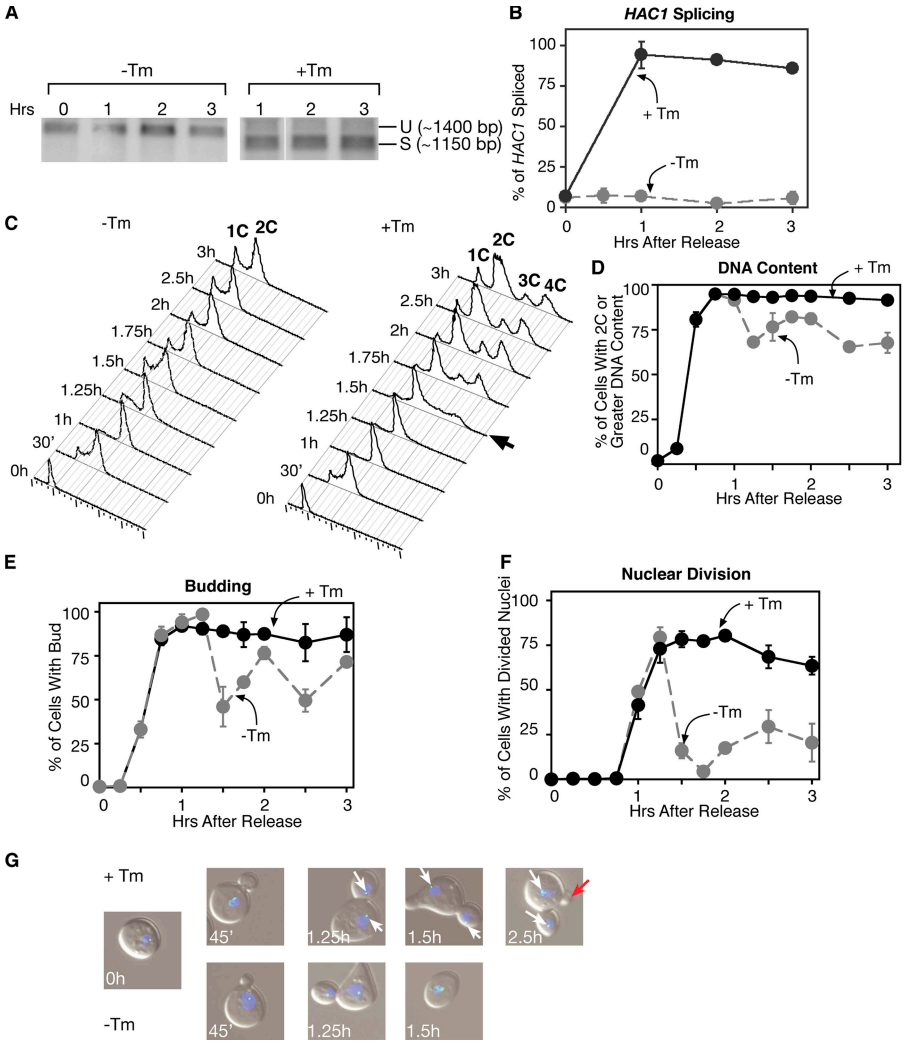

Figure 3. **Tm-treated cells are delayed in the cell cycle with high DNA content, large buds, and divided nuclei.** Wild-type (MNY1005) cells were synchronized with α factor and treated with +/− Tm 30 min after α-factor release (Fig. S3, available at http://www.jcb.org/cgi/content/full/jcb.200702101/DC1). Indicated time points refer to time after α-factor release. (A) Northern analysis with a *HAC1*-specific probe shows the conversion of unspliced *HAC1* mRNA (U) to spliced *HAC1* mRNA (S) in cells experiencing ER stress. (B) Quantitation of A calculated as spliced *HAC1* mRNA divided by total *HAC1* mRNA. (C) Flow cytometric analysis of cells stained with Sytox green to measure DNA content. The arrow indicates the appearance of 3C cells. (D) Quantitation from C of the percentage of cells in the population that contained 2C or greater DNA content. (E) Percentage of total cells that were budded during synchronized growth +/− Tm. (F) Percentage of total cells that contained divided nuclei with properly segregated sister chromatids during synchronized growth +/− Tm. (G) Pictures show DAPI-stained nuclei (blue) and GFP-marked sister chromatids (indicated by white arrows). The red arrow indicates an additional bud. All error bars represent the SD of three repeats. The 15-min difference in wild-type cell division time (1.25 vs. 1.5 h), as assayed by flow cytometry versus the budding index (compare B with C), is likely the result of differences in the cell fixing protocol for the different assays (see Materials and methods).

sister chromatids, indicating that mitosis occurred properly in these Tm-treated cells (Fig. 3 G, white arrows denote GFP-marked chromosomes). Therefore, similar to *ero1-1* cells grown at the restrictive temperature, cells experiencing ER stress as a result of Tm treatment were delayed with a budded morphology after nuclear division.

Tm treatment and *ero1-1*-restrictive growth had very similar effects on the cell cycle, strongly suggesting that these effects are the specific result of ER stress rather than ER-independent effects of Tm treatment or the *ero1-1* allele. To verify that the cell cycle is sensitive specifically to ER stress, we examined the effects of Tm treatment on the cell cycle of synchronized *hac1*Δ cells. Because *HAC1* is required for recovery from ER stress, *hac1*Δ cells should be unable to recover from any specific effect of ER stress but should respond normally to ER-independent stimuli. Indeed, the absence of *HAC1* rendered cells incapable of recovering from the Tm-induced appearance of cells with a high DNA content. The percentage of 3C/4C cells in the wild-type Tm-treated populations peaked at 40% after 2 h of growth (see Fig. 5, A and B) and then began to decline, reaching 25% after 3 h of growth. In contrast, *hac1*Δ cells continued to be 40–45% 3C/4C for the entire 3-h time course.

ER stress induces cytokinesis delay

To distinguish between the possibilities of a late M-phase delay or a delay in cytokinesis, we examined the effect of ER stress on several mitotic events: Clb2p production/degradation, Cdc14p release, and mitotic spindle formation/depolymerization. Clb2p is a major regulator of cell cycle progression. Its levels increase as cells enter mitosis and decrease as cells exit mitosis. Cells delayed in mitotic exit typically display sustained high levels of Clb2p (Mendenhall and Hodge, 1998). Directly after the temperature shift (0-h time point), both wild-type and *ero1-1* cells contained very low levels of Clb2p (Fig. 4 A), which is consistent with most cells being in G1 or S phase. In both cell types, Clb2p levels began to increase 30 min after the temperature shift, marking mitotic entry 15 min before nuclear division (Figs. 3 F and 4 A). Similarly, Clb2p degradation, marking mitotic exit, occurred at the same time (60 min) in wild-type and *ero1-1* cells. In wild-type cells, this Clb2p decrease correlated well with the onset of cytokinesis (Figs. 3 E and 4 A), but, in *ero1-1* cells, cytokinesis did not occur.

The key events of mitotic exit are signaled by the phosphatase Cdc14p, which is only active during anaphase. During all other times in the cell cycle, Cdc14p is kept inactive by virtue of its nucleolar localization. After nuclear division, Cdc14p

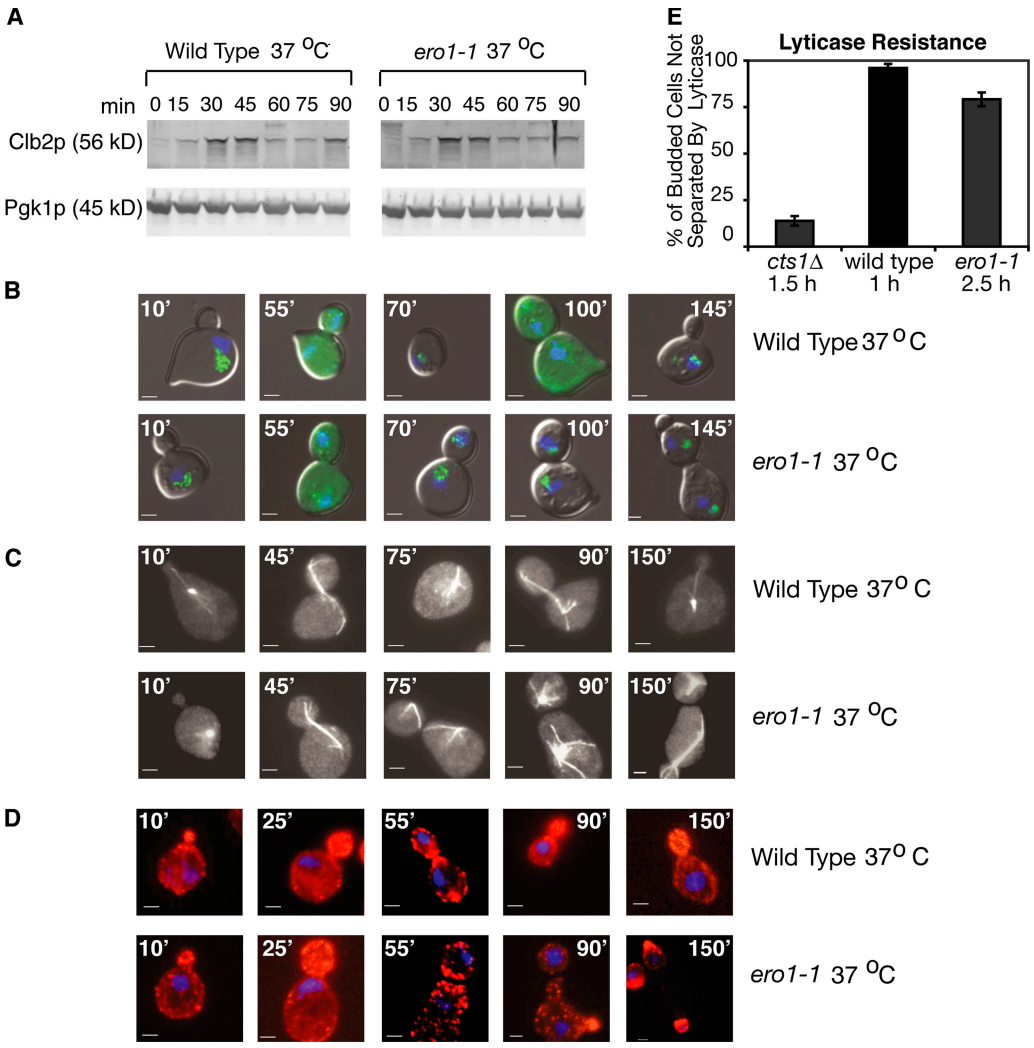

Figure 4. **Ero1p inactivation causes cytokinesis delay.** (A–D) Experiments were performed according to the schematic in Fig. 1 A, and cells were collected for immunoblot analysis, probing for Pgk1p (loading control) and Clb2p (A), Cdc14p-GFP visualization (B), Tub1p-GFP visualization (C), and Alexa-Fluor546-phalloidin staining to visualize actin patch localization (D). Blue indicates DAPI staining. Bars, 2 μm. (E) Wild-type (MNY1002), *cts1Δ* (MNY1012), and *ero1-1* (MNY1003) cells were α-factor synchronized and released at 30 (wild type and *cts1Δ*) or 37°C (*ero1-1*). Cells were grown for the indicated times, and α factor was added back to the medium to prevent second cell cycle initiation. Cells were fixed, and the budding index was calculated before and after lyticase treatment. The graph depicts lyticase resistance, which was calculated as the budding index after lyticase treatment divided by the budding index before lyticase treatment. Error bars represent the SD of three repeats.

is released into the nucleus and cytoplasm, where it signals multiple key cell cycle events, including the completion of Clb2 degradation, breakdown of the mitotic spindle, and cytokinesis (Shou et al., 1999; Stegmeier and Amon, 2004).

10 min after temperature shift, for both wild-type and *ero1-1* cells, Cdc14p-GFP colocalized with a portion of the nucleus, which is consistent with the expected nucleolar localization of Cdc14p (Fig. 4 B). After 55 min of 37°C growth, both cell types released Cdc14p-GFP into their nucleus and cytoplasm, demonstrating that these conditions of ER stress did not delay Cdc14p release. Wild-type cells divided and resumed the nucleolar localization of Cdc14p by 70 min. Mutant cells also reabsorbed Cdc14p into the nucleolus at the 70-min time point but did not divide and eventually assumed a multibudded morphology (Figs. 3 G and 4 B).

Finally, we used a *TUB1*-GFP fusion gene (Straight et al., 1997) to examine the formation and breakdown of the mitotic spindle during ER stress. By 45 min after the temperature shift, both wild-type and *ero1-1* cells exhibited fully formed mitotic spindles between their two spindle pole bodies, indicating that ER stress did not delay spindle formation. Spindle breakdown also occurred at the same time (75 min) in both cell types. Again, *ero1-1* cells did not divide. In the absence of cell division, some *ero1-1* cells rereplicated their spindle pole bodies, rebudded, and reformed a mitotic spindle, thus forming the unusual cells depicted in Fig. 4 C (150′ panel).

We also examined Clb2 fluctuations, Cdc14p release, and mitotic spindle formation and breakdown in synchronized untreated and Tm-treated cells. We found that like *ero1-1*, Tm had no effect on these mitotic markers (Fig. S4, available at http://www.jcb.org/cgi/content/full/jcb.200702101/DC1). Therefore, ER stress delays cell division but does not affect mitotic entry, mitosis, or mitotic exit, suggesting that ER stress specifically inhibits cytokinesis or cell separation.

Cytokinesis creates a membrane barrier between mother and daughter cells. After cytokinesis, the septum continues to hold the two cells together; the septum must be degraded for cell separation to occur (Yeong, 2005). Experimentally, lyticase can be used to degrade the septum of delayed cells, thus differentiating between a cytokinesis defect and a defect in cell separation.

Lyticase treatment demonstrated that ER-stressed cells fail to divide because of incomplete cytokinesis rather than incomplete cell separation. We collected *ero1-1* cells 2.5 h after temperature shift as described in Fig. 2 A except that α factor was added back to the medium 45 min after G1 release to prevent the initiation of a second cell cycle. As before, most cells were delayed with a budded morphology at this time point. Their delay was clearly caused by a cytokinesis defect, as 79% of these budded cells were resistant to cell separation by lyticase treatment (Fig. 4 E). Confirming that lyticase treatment only separated cells that had completed cytokinesis, wild-type cells in M phase (collected 1 h after α-factor release) remained 96% budded after lyticase treatment. In addition, *cts1Δ* cells, which are known to be defective in cell separation (Kuranda and Robbins, 1991), were 43% budded 1.5 h after α-factor release (unpublished data). Of the budded *cts1Δ* cells, 86% were separated by lyticase (Fig. 4 E), confirming that the experimental conditions used here were sufficient to dissociate the majority of separation-defective cells.

Successful cytokinesis requires that cortical actin patches become polarized to either side of the bud neck late in the cell cycle (Kilmartin and Adams, 1984; Novick and Botstein, 1985; Mulholland et al., 1994; Doyle and Botstein, 1996; Waddle et al., 1996). We followed actin patch localization in synchronized cells and found that wild-type and *ero1-1* cells displayed bud-localized cortical actin patches throughout S, G2, and most of M phase (Fig. 4 D). Just before cytokinesis, the actin patches of *ero1-1* cells redistributed to the bud neck in a manner indistinguishable from wild-type cells (Fig. 4 D). Therefore, the ER stress–induced cytokinesis defect is not caused by a delay or alteration in actin patch redistribution.

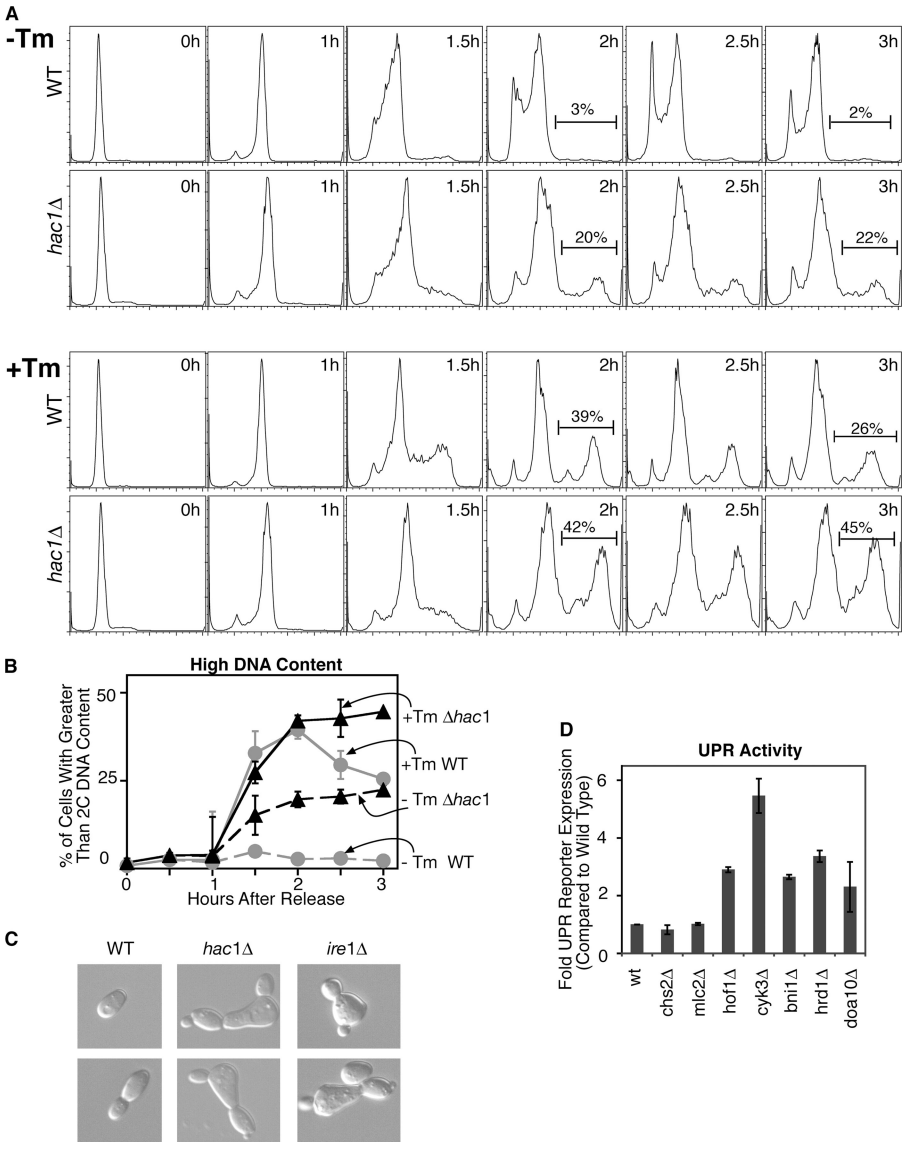

Figure 5. **UPR signaling facilitates cytokinesis during normal cell growth.** (A) Wild-type (MNY1002) and *hac1*Δ (MNY1010) cells were treated with +/− Tm 30 min after α-factor release. Cells were fixed, stained with Sytox green, and analyzed by flow cytometry. Bars define a subpopulation of high DNA content cells, and the given numbers indicate percentages of the total live cell population that has a high DNA content. (B) Quantitation of A. (C) Wild type (WT; MNY1002), *hac1*Δ (MNY1010), and *ire*Δ (MNY1011) were released from α-factor arrest for 3 h before fixation and microscopic examination. (D) Wild type (RHY2724), *hrd1Δ* (RHY5088), *hof1Δ* (RHY5954), *chs2Δ* (RHY5955), *cyk3Δ* (RHY5956), *mlc2Δ* (RHY5957), *doa10Δ* (RHY5958), and *bni1Δ* (RHY5959) cells, which expressed a 4× UPRE-GFP reporter construct, were analyzed by flow cytometry to measure UPR activity in the absence of externally induced ER stress. Graphs represent fold induction compared with wild-type cells. All error bars represent the SD of three repeats.

UPR signaling facilitates cytokinesis during normal cell growth

The induction of ER stress in synchronized cell populations revealed that cytokinesis is highly sensitive to the state of the ER. This suggests that ER capacity increases during cell division, a process that might be facilitated by UPR signaling. To determine whether UPR signaling affects cytokinesis during normal cell growth, we examined cytokinesis in *hac1*Δ strains. In the absence of any external ER stressor, wild-type cell populations never exhibited cells with a >2C DNA content. In contrast, after 1.5 h of normal synchronized growth, 15% of untreated *hac1*Δ cells were >2C. This number increased to 20% after 2 h of growth and remained ∼20% until the end of the 3-h time course (Fig. 5 A). Untreated *hac1Δ* cells were almost as cytokinesis deficient as wild-type cells treated with Tm (Fig. 5 A, compare wild-type +Tm to *hac1*Δ −Tm). Furthermore, we examined *hac1Δ* and *ire1Δ* strains for the multibudded morphology that is indicative of cells with a cytokinesis defect. We found that a small percentage of cells (<1%) did display this multibudded morphology, whereas we never observed multibudded cells in wild-type populations (Fig. 5 C). A complete cytokinesis block should cause a much higher percentage of cells to attain multiple buds. Therefore, UPR mutants are delayed in cytokinesis rather than blocked.

To further investigate the link between UPR signaling and the cytokinesis process, we measured basal UPR activity in various cytokinesis mutants using a 4× UPRE-GFP reporter construct (Pollard et al., 1998). *MLC2*, *CHS2*, *HOF1*, *CYK3*, and *BNI1* all participate in cytokinesis (see Discussion). Of the cytokinesis mutants tested, *mlc2Δ* and *chs2Δ* strains did not exhibit basal UPR activity (Fig. 5 D). However, in the absence of any external ER stress induction, *hof1Δ*, *cyk3Δ*, and *bni1Δ* strains exhibited three- to sixfold UPR reporter gene expression compared with wild-type cells. This level of reporter activity reflects a true link between the UPR and cytokinesis, as *hrd1Δ* and *doa10Δ* mutants, which are ERAD deficient and are known to induce functionally relevant levels of UPR activity (Travers et al., 2000; Swanson et al., 2001), exhibited similar levels of reporter gene expression. The finding that some cytokinesis mutants exhibit UPR activation is quite novel: the detection of basal UPR activity has been previously limited to mutants with specific ER defects.

Discussion

A housekeeping function for the UPR: how the ER adapts to normal fluctuations in cellular demand

In eukaryotic cells, critical cellular functions are organized and performed by functionally specialized organelles. This compartmentalization of function eases the maintenance of cellular homeostasis, as each organelle can separately control its own function in accordance with the complex requirements of the cell. The ER, for example, has a vital role in the production of lipids and proteins that make up the secretory pathway, plasma membrane, and, in yeast, the cell wall. Even during normal, unstressed growth, different internal cellular conditions, such as different stages of the cell division cycle, probably require different levels of ER functionality. However, the precise mechanism of adapting ER function to suit physiological fluctuations in internal cellular conditions is unknown. Because such a mechanism would be capable of sensing the condition of the ER and adjusting the ER's capacity, the UPR pathway is an excellent candidate for a mechanism of ER adaptation.

In our study, we have shown that cytokinesis requires higher levels of ER functionality than other cell cycle events. This finding implies that ER functionality increases during cytokinesis and allowed us to examine the UPR's role in achieving this functional increase. We found that UPR-deficient strains were cytokinesis defective. In addition, several cytokinesis-defective strains displayed elevated basal UPR activity. Collectively, our data establish a function for the UPR pathway in facilitating cell division during normal cell growth. The UPR presumably achieves this function by adapting ER capacity.

The UPR's role in cytokinesis, which is revealed in this study, represents a novel type of UPR activity, as it can be detected during optimal unstressed growth conditions. All previous studies of UPR mutants describe their inability to respond to unusually stressful growth conditions such as inositol starvation (Nikawa and Yamashita, 1992; Cox et al., 1993), drug treatments that induce widespread protein misfolding (Cox et al., 1993; Mori et al., 1993), overexpression of a misfolded mutant protein (Casagrande et al., 2000; Friedlander et al., 2000; Spear and Ng, 2003), or development into a specialized secretory cell (Reimold et al., 2001; Gass et al., 2002; Iwakoshi et al., 2003; van Anken et al., 2003). Each of these known UPR-requiring conditions imposes a massive load on the ER. The newly discovered importance of UPR signaling during normal cell growth uncovers a novel housekeeping function for the UPR pathway. In addition to responding to stressful growth conditions, the UPR must monitor and manage the cell's fluctuating ER requirements.

The UPR's ability to serve a housekeeping function sheds new light on the mode of UPR activation. In theory, the UPR pathway might operate according to one of two modes of activation. It could activate in a manner similar to an on/off switch. In this case, the pathway remains "off" until a threshold level of stress is experienced, at which point the pathway turns "on" and becomes highly active. Alternatively, the UPR pathway might operate as a dimmer switch in which the off state and on state actually represent two extremes on a continuum. Previous studies have investigated the UPR pathway by inducing crisis levels of ER stress (Cox et al., 1993; Mori et al., 1993; Casagrande et al., 2000; Spear and Ng, 2003). If the UPR pathway could fine tune the level of ER function, this could actually prevent such an ER crisis by allowing the gradual adaptation of ER capacity.

Data from previous studies provide support for both modes of activation. In support of the on/off switch mode of activation, *HAC1* mRNA remains unspliced during normal cell growth but becomes rapidly and efficiently spliced upon treatment with DTT or Tm or upon the overexpression of misfolded proteins (Cox and Walter, 1996). In addition, certain modest amounts of ER stress have been shown to not activate the UPR pathway at all. For example, expression of the misfolded mutant protein CPY* from its genomic locus does not activate UPR

signaling, and ERAD of genomic CPY* does not require UPR components (Friedlander et al., 2000). However, data are also accumulating to support the dimmer switch mode of UPR activation. For example, certain mutations in the ERAD pathway have been shown to induce intermediate levels of UPR activity (Cox and Walter, 1996; Friedlander et al., 2000; Travers et al., 2000). Our study further supports the dimmer switch mode of UPR activation, as we have shown that subtle activation of the UPR pathway contributes to efficient cytokinesis.

The ER's role in cytokinesis

Although DNA replication, mitotic entry, spindle formation, nuclear segregation, Cdc14p release, mitotic exit, spindle disassembly, and actin patch repolarization all occur normally during ER stress, cytokinesis does not (summarized in Fig. 6). Therefore, we have found that ER stress specifically disrupts cytokinesis, and we have ruled out the possibility that this disruption is caused by a defect in actin patch relocalization. This disruption could be caused by a stress-induced attenuation of any of the ER's many functions, including secretion, ERAD, or phospholipid metabolism.

Despite the ER's well-characterized role in initiating protein secretion, it remains unknown whether ER stress inhibits the entire secretory pathway. If it does, there are several reasons that this may impact cytokinesis. Cytokinesis begins with the assembly and contraction of an actomyosin ring. In animal cells, it has been shown that membrane deposition at the cleavage furrow must accompany actomyosin ring contraction for proper cytokinesis to occur (Skop et al., 2001; Shuster and Burgess, 2002). The extra membrane, which is delivered in the form of secretory vesicles, presumably relieves the tension created by membrane constriction. Perhaps, as in animal cells, the yeast secretory pathway assists in cytokinesis by providing new membrane to the site of ring contraction, and it is the lack of membrane at the bud neck that prevents cytokinesis under conditions of ER stress.

Regardless of whether membrane addition itself is required for yeast cytokinesis, it is clear that Golgi-derived vesicles are targeted to the yeast bud neck at the end of the cell cycle and that these vesicles assist in the process of cytokinesis. First, vesicles carry cargo that is necessary for actomyosin ring contraction. Cells that are defective in vesicle fusion assemble an actomyosin ring normally, but the assembled ring is unstable and does not properly contract (VerPlank and Li, 2005). Second, during cytokinesis, secretory vesicles provide the yeast bud neck with the enzymes responsible for septum formation, a process that is essential for yeast cytokinesis (Shaw et al., 1991; Valdivia and Schekman, 2003; VerPlank and Li, 2005). Therefore, if ER stress disrupts vesicle trafficking, this could slow membrane deposition, ring contraction, and/or septation and, thereby, delay cytokinesis, thus explaining the results of our study. This explanation implies that during normal cytokinesis, the UPR manifests its housekeeping function by increasing the cell's secretory capacity, thus fulfilling the enhanced secretory requirements of cytokinesis.

Despite expectations that ER stress would broadly inhibit secretion, some studies find that ER stress has a minimal impact,

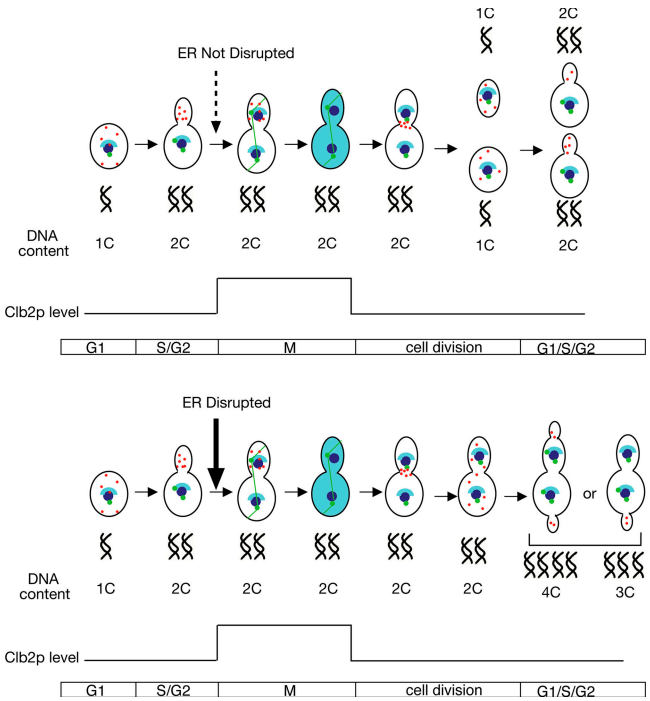

Figure 6. **Summary of results.** When the ER is perturbed (*ero1-1*-restrictive growth or Tm treatment), budding, DNA replication, Clb2p synthesis, spindle formation, nuclear division, Cdc14p release, Clb2p degradation, spindle breakdown, and actin repolarization occur at the same time as unstressed cells. However, *ero1-1*-restrictive growth and Tm treatment delay cytokinesis, resulting in the formation of cells with extra buds and high DNA content. Green, tubulin; red, actin; dark blue, nucleus; light blue, Cdc14p.

if any, on the overall secretory pathway (Casagrande et al., 2000; Spear and Ng, 2003). This suggests that the ER might play a role in cytokinesis through one of its cellular functions besides protein folding and trafficking. This possibility is especially intriguing, as it implies that the UPR pathway can detect ER functional cues other than the simple accumulation of unfolded proteins in the ER. Although previous studies have not tested this prospect directly, UPR target genes represent the entire spectrum of ER functions (Travers et al., 2000).

In addition to functioning in protein folding and secretion, the ER has the task of regulating phospholipid metabolism. Because cytokinesis entails a membrane fusion event and the creation of a membrane barrier between mother cell and daughter cell, it is not surprising that certain phospholipids are necessary for its proper completion. Phosphatidylethanolamine and phosphatidylinositol 4,5-bisphosphate become locally concentrated to the cleavage furrow during cytokinesis in various eukaryotic cell types. Interfering with the production of either of these two phospholipids results in a cytokinesis defect (Brill et al., 2000; Emoto and Umeda, 2001; Emoto et al., 2005; Janetopoulos and Devreotes, 2006). Therefore, the disruption of cytokinesis by ER stress may be caused by the effects of ER stress on phospholipid metabolism. If this is the case, the UPR's role during normal cytokinesis may be to up-regulate genes involved in phospholipid metabolism.

Three cytokinesis mutants, *bni1Δ*, *hof1Δ*, and *cyk3Δ*, exhibit constitutive UPR activity. Strains deleted for *MLC2*

Table I. **Yeast strains used in this study**

Strain	Relevant genotype	Source
MNY1000	*MATa, leu2-3,112, trp1-1, can1-100, ura3-1, ade2-1, his3-11,15*	Cox et al., 1993
MNY1001	*MATa, leu2-3,112, trp1-1, can1-100, ura3-1, ade2-1, his3-11,15, ero1-1::HIS3*	Frand and Kaiser, 1998
MNY1002	*MATa, leu2-3,112, trp1-1, can1-100, ura3-1, ade2-1, his3-11,15::HIS3, bar1::LEU2*	This study
MNY1003	*MATa, leu2-3,112, trp1-1, can1-100, ura3-1, ade2-1, his3-11,15, ero1-1::HIS3, bar1::LEU2*	This study
MNY1004	*MATa, leu2-3,112, trp1-1, can1-100, ura3-1, ade2-1, his3-11,15::UPRE-lacZ:HIS3*	Cox et al., 1993
MNY1005	*MATa, leu2-3,112, trp1-1::lacO:TRP1, can1-100, ura3-1, ade2-1, his3-11, 15::pCUP1-GFP12-LacI12:HIS3, bar1Δ*	Biggins et al., 1999
MNY1006	*MATa, leu2-3,112, trp1-1, can1-100, ura3-1, ade2-1, his3-11,15::HIS3, bar1::LEU2, CDC14-GFP::KanMX*	This study
MNY1007	*MATa, leu2-3,112, trp1-1, can1-100, ura3-1, ade2-1, his3-11,15, bar1::LEU2, ero1-1::HIS3, CDC14-GFP::KanMX*	This study
MNY1008	*MATa, leu2-3,112, trp1-1, can1-100, ura3-1::TUB1-GFP:URA3, ade2-1, his3-11,15::HIS3, bar1::LEU2*	This study
MNY1009	*MATa, leu2-3,112, trp1-1, can1-100, ura3-1::TUB1-GFP:URA3, ade2-1, his3-11,15, bar1::LEU2, ero1-1::HIS3*	This study
MNY1010	*MATa, leu2-3,112, trp1-1, can1-100, ura3-1, ade2-1, his3-11,15::HIS3, bar1::LEU2, hac1Δ::KanMX*	This study
MNY1011	*MATa, leu2-3,112, trp1-1, can1-100, ura3-1, ade2-1, his3-11,15::HIS3, bar1::LEU2, ire1Δ::KanMX*	This study
MNY1012	*MATa, leu2-3,112, trp1-1, can1-100, ura3-1, ade2-1, his3-11,15::HIS3, bar1::LEU2, cts1Δ::KanMX*	This study
RHY2724	*MATα, met2, lys2-801, ura3-52::4xUPRE-GFP:URA3, ade2-101, his3Δ200*	This study
RHY5088	*MATα, met2, lys2-801, ura3-52::4xUPRE-GFP:URA3, ade2-101, his3Δ200, hrd1Δ::KanMX*	This study
RHY5954	*MATα, met2, lys2-801, ura3-52::4xUPRE-GFP:URA3, ade2-101, his3Δ200, hof1Δ::KanMX*	This study
RHY5955	*MATα, met2, lys2-801, ura3-52::4xUPRE-GFP:URA3, ade2-101, his3Δ200, chs2Δ::KanMX*	This study
RHY5956	*MATα, met2, lys2-801, ura3-52::4xUPRE-GFP:URA3, ade2-101, his3Δ200, cyk3Δ::KanMX*	This study
RHY5957	*MATα, met2, lys2-801, ura3-52::4xUPRE-GFP:URA3, ade2-101, his3Δ200, mlc2Δ::KanMX*	This study
RHY5958	*MATα, met2, lys2-801, ura3-52::4xUPRE-GFP:URA3, ade2-101, his3Δ200, doa10Δ::NatMX*	This study
RHY5959	*MATα, met2, lys2-801, ura3-52::4xUPRE-GFP:URA3, ade2-101, his3Δ200, bni1Δ::NatMX*	This study

or *CHS2*, which are involved in the cytokinesis processes of actomyosin ring disassembly and septum formation, respectively (Shaw et al., 1991; Luo et al., 2004), did not activate the UPR. During yeast cytokinesis, *BNI1* promotes actomyosin ring assembly (Tolliday et al., 2002), *HOF1* coordinates ring contraction with septum formation (Lippincott and Li, 1998; Luo et al., 2004), and *CYK3* mediates septum formation (Korinek et al., 2000). There is no indication that any of these mutants are defective in protein secretion or any other aspect of ER function. This is the first instance of UPR activity in mutants that are not directly defective in an ER-associated function. Furthermore, unlike previous cases of basal UPR activity in mutants, none of these three genes is a UPR target gene (Travers et al., 2000). Therefore, the UPR induction in these mutants does not represent the cell's attempt to transcriptionally activate the specific gene that is absent. Increased UPR activity in *hof1Δ*, *cyk3Δ*, and *bni1Δ* strains probably helps these cells partially overcome their cytokinesis defect. This implies that the UPR pathway can directly or indirectly sense and modify the cell's cytokinesis efficiency.

Our data highlight a new role for the UPR pathway in cytokinesis. Cytokinesis probably represents only one of many normal cellular functions that invoke a moderate level of UPR induction. Although difficult to detect, these instances of moderate UPR induction could help the ER constantly maintain an appropriate capacity in a fluctuating cellular environment.

Materials and methods

Strains, media, growth conditions, and synchronization

Yeast strains containing MNY numbers were in the W303 strain background, and strains containing RHY numbers were derived from the S288C strain background. All strains were generated using standard genetic methods and are listed in Table I. MNY1008 and MNY1009 were constructed by integrating StuI-linearized pAFS125 (Straight et al., 1997) at the *URA3* locus. All strains carrying the UPRE-GFP reporter were constructed by integrating StuI-linearized pJCI86-GFP (Pollard et al., 1998) at the *URA3* locus. Wild-type and *ero1-1* CDC14-GFP strains were constructed using a one-step PCR-mediated technique (Longtine et al., 1998). All deletion strains were constructed by amplification of the Research Genetics heterozygous diploid collection followed by G418 selection and verification by PCR.

Cells were grown in YPD medium (1% yeast extract, 2% bactopeptone, and 2% glucose) at 30°C unless otherwise noted. All strains carrying the 4× UPRE-GFP reporter construct were grown in synthetic complete –URA medium at 30°C. For synchronization, α factor (stored as 1-mg/ml stock in PBS at –20°C) was added to early log-phase cultures to a final concentration of 50 ng/ml for 2.5 h (30°C growth conditions) or 3 h (25°C growth conditions). To release cells from α-factor arrest, cells were collected by centrifugation, washed twice with an equal volume of medium, and resuspended in fresh medium to an OD of 0.25. Tm was stored as 10-mg/ml stock in DMSO and added to cells at a final concentration of 1 μg/ml. During Tm experiments, 0.1% DMSO was added to untreated cells to control for effects of the vehicle.

Cell extracts, Northern blotting, and immunoblotting

For Western blot analysis, ~3×10^7 cells were harvested by centrifugation at 4°C, washed with 1 ml H_2O, frozen with liquid N_2, and stored at –80°C. Pellets were resuspended in 100 μl of lysis buffer (50 mM Tris-HCl, pH 7.5, 150 mM NaCl, 5 mM EDTA, 1% NP-40, 1 mM sodium pyrophosphate, 1 mM PMSF, 1 mM sodium orthovanadate, 2 μg/ml pepstatin A,

2 μg/ml leupeptin, 20 mM NaF, 5 μg/ml aprotinin, and 1.75 mM β-glycerophosphate). 100 μl of acid-washed glass beads were added, and cells were vortexed at 4°C for 5 min. Lysates were centrifuged at 13,000 *g* for 8 min at 4°C, and the supernatant was collected. Protein concentration was determined using a BCA protein assay kit (Pierce Chemical Co.). 30 μg of protein was denatured at 95°C in 2× loading buffer (125 mM Tris-HCl, pH 6.8, 2% SDS, 50% glycerol, 12% β-mercaptoethanol, and 0.02% bromophenol blue) and was loaded on a 10% SDS-polyacrylamide gel (Invitrogen). Clb2p was detected with a 1:1,000 dilution of anti-Clb2 antibody (Santa Cruz Biotechnology, Inc.) followed by anti–rabbit secondary antibody at a dilution of 1:10,000 (GE Healthcare) and ECL detection (GE Healthcare). RNA isolation and *HAC1* Northern blotting were performed essentially as described previously (Cox and Walter, 1996) and were quantified using a phosphorimager (Typhoon; GE Healthcare).

DNA staining and flow cytometry

Approximately 10^7 cells were collected by centrifugation at 4°C, washed with 1 ml of ice-cold H_2O, and resuspended in 400 μl of cold H_2O. 1 ml of ice-cold EtOH was added slowly, and cells were fixed at 4°C overnight or longer. After fixation, cells were collected by centrifugation, washed with 1 ml PBS, and treated with 1 mg/ml RNase A in 100 μl PBS at 37°C for 2–12 h. Cells were then treated with 5 mg/ml pepsin in 200 μl H_2O, pH 2.0, at 37°C for 20 min followed by washing and resuspension in 1 ml PBS. Cells were sonicated for 15 s at 15%. 100 μl of cells (10^6 cells) were stained with 1 μM Sytox green (Invitrogen) in PBS. Data were collected using a flow cytometer (FACSCalibur; BD Biosciences) and analyzed using FlowJo software (Tree Star).

Strains carrying the 4× UPRE-GFP reporter construct were analyzed for UPR induction by measuring GFP fluorescence in live log-phase cells with a FACSCalibur flow cytometer. The mean fluorescence for each strain was divided by the mean fluorescence of an isogenic wild-type strain to calculate fold induction.

Microscopy

Cells were fixed in 4% PFA and sonicated briefly before analysis. Budding index was calculated as the number of cells with an obvious bud divided by the total number of cells counted. For visualization of nuclei, DAPI was added to a concentration of 0.04 μg/ml. Nuclear division was scored as positive when two separate DAPI bodies were present in a single cell. To visualize sister chromatid segregation, MNY1005 cells expressed a LacI12-GFP fusion protein and contained a Lac operon at the TRP1 locus. This caused both copies of chromosome IV to be GFP marked (Biggins et al., 1999). For the visualization of actin, cells were fixed in 4% PFA/PBS, washed with PBS, and incubated with 6.6 μM AlexaFluor546-phalloidin (Invitrogen). All cells were visualized using a microscope (Axiovert 200M; Carl Zeiss MicroImaging, Inc.) with a 100× 1.3 NA objective. Images were captured using a monochrome digital camera (Axiocam; Carl Zeiss MicroImaging, Inc.) and analyzed using Axiovision software (Carl Zeiss MicroImaging, Inc.).

Lyticase treatment

Cells were fixed in YPD/4% formaldehyde for 10 min followed by 1 h in 400 mM $KHPO_4$, pH 6.5, 500 μM $MgCl_2$, and 4% formaldehdye. Cells were then washed in 400 mM $KHPO_4$, pH 6.5, and 500 μM $MgCl_2$ and resuspended in 400 mM $KHPO_4$, pH 6.5, 500 μM $MgCl_2$, and 1 M sorbitol. Fixed cells were sonicated (15% for 15 s) and treated with 80 U/ml lyticase at 37°C for 1 h.

Online supplemental material

Fig. S1 shows by RT-PCR that spliced *HAC1* mRNA is present in unstressed wild-type cells but not in *ire1Δ* cells. Fig. S2 shows that asynchronous *ero1-1* cells accumulate with a 2C or greater DNA content when shifted to restrictive growth. Fig. S3 demonstrates that Tm inhibits budding when added directly after α-factor release but has no effect on DNA replication. This budding inhibition is bypassed when Tm is added 30 min after α-factor release. Fig. S4 shows that Tm treatment does not affect Clb2p production/degradation, Cdc14p release, mitotic spindle formation/depolymerization, or actin patch relocalization but still inhibits cytokinesis. Online supplemental material is available at http://www.jcb.org/cgi/content/full/jcb.200702101/DC1.

We are grateful to Randy Hampton, Arshad Desai, and Lorraine Pillus for reagents and for scientific discussion. We also thank Randy Hampton for critical reading of the manuscript, Steven Reed for scientific advice, and Chris Kaiser for providing the *ero1-1* strain.

A. Bicknell was supported by the National Science Foundation Graduate Research Fellowship. M. Niwa was supported by grants from the Searle Scholar Program, the University of California, the Cancer Research Committee, and the American Cancer Society.

Submitted: 15 February 2007
Accepted: 15 May 2007

References

Arnold, E., and W. Tanner. 1982. An obligatory role of protein glycosylation in the life cycle of yeast cells. *FEBS Lett.* 148:49–53.

Biggins, S., F.F. Severin, N. Bhalla, I. Sassoon, A.A. Hyman, and A.W. Murray. 1999. The conserved protein kinase Ipl1 regulates microtubule binding to kinetochores in budding yeast. *Genes Dev.* 13:532–544.

Brill, J.A., G.R. Hime, M. Scharer-Schuksz, and M.T. Fuller. 2000. A phospholipid kinase regulates actin organization and intercellular bridge formation during germline cytokinesis. *Development*. 127:3855–3864.

Casagrande, R., P. Stern, M. Diehn, C. Shamu, M. Osario, M. Zuniga, P.O. Brown, and H. Ploegh. 2000. Degradation of proteins from the ER of *S. cerevisiae* requires an intact unfolded protein response pathway. *Mol. Cell*. 5:729–735.

Chapman, R., C. Sidrauski, and P. Walter. 1998. Intracellular signaling from the endoplasmic reticulum to the nucleus. *Annu. Rev. Cell Dev. Biol.* 14:459–485.

Cox, J.S., and P. Walter. 1996. A novel mechanism for regulating activity of a transcription factor that controls the unfolded protein response. *Cell*. 87:391–404.

Cox, J.S., C.E. Shamu, and P. Walter. 1993. Transcriptional induction of genes encoding endoplasmic reticulum resident proteins requires a transmembrane protein kinase. *Cell*. 73:1197–1206.

Daum, G., N.D. Lees, M. Bard, and R. Dickson. 1998. Biochemistry, cell biology and molecular biology of lipids of *Saccharomyces cerevisiae*. *Yeast*. 14:1471–1510.

Doyle, T., and D. Botstein. 1996. Movement of yeast cortical actin cytoskeleton visualized in vivo. *Proc. Natl. Acad. Sci. USA*. 93:3886–3891.

Ellgaard, L., M. Molinari, and A. Helenius. 1999. Setting the standards: quality control in the secretory pathway. *Science*. 286:1882–1888.

Emoto, K., and M. Umeda. 2001. Membrane lipid control of cytokinesis. *Cell Struct. Funct.* 26:659–665.

Emoto, K., H. Inadome, Y. Kanaho, S. Narumiya, and M. Umeda. 2005. Local change in phospholipid composition at the cleavage furrow is essential for completion of cytokinesis. *J. Biol. Chem.* 280:37901–37907.

Frand, A.R., and C.A. Kaiser. 1998. The ERO1 gene of yeast is required for oxidation of protein dithiols in the endoplasmic reticulum. *Mol. Cell*. 1:161–170.

Frand, A.R., and C.A. Kaiser. 1999. Ero1p oxidizes protein disulfide isomerase in a pathway for disulfide bond formation in the endoplasmic reticulum. *Mol. Cell*. 4:469–477.

Friedlander, R., E. Jarosch, J. Urban, C. Volkwein, and T. Sommer. 2000. A regulatory link between ER-associated protein degradation and the unfolded-protein response. *Nat. Cell Biol.* 2:379–384.

Gass, J.N., N.M. Gifford, and J.W. Brewer. 2002. Activation of an unfolded protein response during differentiation of antibody-secreting B cells. *J. Biol. Chem.* 277:49047–49054.

Haase, S.B., and S.I. Reed. 2002. Improved flow cytometric analysis of the budding yeast cell cycle. *Cell Cycle*. 1:132–136.

Hampton, R.Y. 2002. ER-associated degradation in protein quality control and cellular regulation. *Curr. Opin. Cell Biol.* 14:476–482.

Harding, H.P., H.Q. Zeng, Y.H. Zhang, R. Jungries, P. Chung, H. Plesken, D.D. Sabatini, and D. Ron. 2001. Diabetes mellitus and exocrine pancreatic dysfunction in Perk- mice reveals a role for translational control in secretory cell survival. *Mol. Cell*. 7:1153–1163.

Hartwell, L.H. 1974. *Saccharomyces cerevisiae* cell cycle. *Bacteriol. Rev.* 38:164–198.

Iwakoshi, N.N., A.H. Lee, P. Vallabhajosyula, K.L. Otipoby, K. Rajewsky, and L.H. Glimcher. 2003. Plasma cell differentiation and the unfolded protein response intersect at the transcription factor XBP-1. *Nat. Immunol.* 4:321–329.

Janetopoulos, C., and P. Devreotes. 2006. Phosphoinositide signaling plays a key role in cytokinesis. *J. Cell Biol.* 174:485–490.

Kaufman, R.J. 2002. Orchestrating the unfolded protein response in health and disease. *J. Clin. Invest.* 110:1389–1398.

Kawahara, T., H. Yanagi, T. Yura, and K. Mori. 1997. Endoplasmic reticulum stress-induced mRNA splicing permits synthesis of transcription factor Hac1p/Ern4p that activates the unfolded protein response. *Mol. Biol. Cell*. 8:1845–1862.

Kilmartin, J.V., and A.E. Adams. 1984. Structural rearrangements of tubulin and actin during the cell cycle of the yeast *Saccharomyces*. *J. Cell Biol.* 98:922–933.

Korinek, W.S., E. Bi, J.A. Epp, L. Wang, J. Ho, and J. Chant. 2000. Cyk3, a novel SH3-domain protein, affects cytokinesis in yeast. *Curr. Biol.* 10:947–950.

Kuranda, M.J., and P.W. Robbins. 1991. Chitinase is required for cell separation during growth of *Saccharomyces cerevisiae*. *J. Biol. Chem.* 266:19758–19767.

Lippincott, J., and R. Li. 1998. Dual function of Cyk2, a cdc15/PSTPIP family protein, in regulating actomyosin ring dynamics and septin distribution. *J. Cell Biol.* 143:1947–1960.

Longtine, M.S., A. McKenzie III, D.J. Demarini, N.G. Shah, A. Wach, A. Brachat, P. Philippsen, and J.R. Pringle. 1998. Additional modules for versatile and economical PCR-based gene deletion and modification in *Saccharomyces cerevisiae*. *Yeast*. 14:953–961.

Luo, J., E.A. Vallen, C. Dravis, S.E. Tcheperegine, B. Drees, and E. Bi. 2004. Identification and functional analysis of the essential and regulatory light chains of the only type II myosin Myo1p in *Saccharomyces cerevisiae*. *J. Cell Biol.* 165:843–855.

McMillan, J.N., R.A. Sia, and D.J. Lew. 1998. A morphogenesis checkpoint monitors the actin cytoskeleton in yeast. *J. Cell Biol.* 142:1487–1499.

Mendenhall, M.D., and A.E. Hodge. 1998. Regulation of Cdc28 cyclin-dependent protein kinase activity during the cell cycle of the yeast *Saccharomyces cerevisiae*. *Microbiol. Mol. Biol. Rev.* 62:1191–1243.

Mori, K. 2000. Tripartite management of unfolded proteins in the endoplasmic reticulum. *Cell*. 101:451–454.

Mori, K., W. Ma, M.J. Gething, and J. Sambrook. 1993. A transmembrane protein with a cdc2+/CDC28-related kinase activity is required for signaling from the ER to the nucleus. *Cell*. 74:743–756.

Mulholland, J., D. Preuss, A. Moon, A. Wong, D. Drubin, and D. Botstein. 1994. Ultrastructure of the yeast actin cytoskeleton and its association with the plasma membrane. *J. Cell Biol.* 125:381–391.

Nikawa, J., and S. Yamashita. 1992. IRE1 encodes a putative protein kinase containing a membrane-spanning domain and is required for inositol phototrophy in *Saccharomyces cerevisiae*. *Mol. Microbiol.* 6:1441–1446.

Novick, P., and D. Botstein. 1985. Phenotypic analysis of temperature-sensitive yeast actin mutants. *Cell*. 40:405–416.

Patil, C., and P. Walter. 2001. Intracellular signaling from the endoplasmic reticulum to the nucleus: the unfolded protein response in yeast and mammals. *Curr. Opin. Cell Biol.* 13:349–355.

Pollard, M.G., K.J. Travers, and J.S. Weissman. 1998. Ero1p: a novel and ubiquitous protein with an essential role in oxidative protein folding in the endoplasmic reticulum. *Mol. Cell*. 1:171–182.

Reimold, A.M., N.N. Iwakoshi, J. Manis, P. Vallabhajosyula, E. Szomolanyi-Tsuda, E.M. Gravallese, D. Friend, M.J. Grusby, F. Alt, and L.H. Glimcher. 2001. Plasma cell differentiation requires the transcription factor XBP-1. *Nature*. 412:300–307.

Ruegsegger, U., J.H. Leber, and P. Walter. 2001. Block of HAC1 mRNA translation by long-range base pairing is released by cytoplasmic splicing upon induction of the unfolded protein response. *Cell*. 107:103–114.

Shamu, C.E., and P. Walter. 1996. Oligomerization and phosphorylation of the Ire1p kinase during intracellular signaling from the endoplasmic reticulum to the nucleus. *EMBO J.* 15:3028–3039.

Shaw, J.A., P.C. Mol, B. Bowers, S.J. Silverman, M.H. Valdivieso, A. Duran, and E. Cabib. 1991. The function of chitin synthases 2 and 3 in the *Saccharomyces cerevisiae* cell cycle. *J. Cell Biol.* 114:111–123.

Shin, D.Y., K. Matsumoto, H. Iida, I. Uno, and T. Ishikawa. 1987. Heat shock response of *Saccharomyces cerevisiae* mutants altered in cyclic AMP-dependent protein phosphorylation. *Mol. Cell. Biol.* 7:244–250.

Shou, W., J.H. Seol, A. Shevchenko, C. Baskerville, D. Moazed, Z.W. Chen, J. Jang, H. Charbonneau, and R.J. Deshaies. 1999. Exit from mitosis is triggered by Tem1-dependent release of the protein phosphatase Cdc14 from nucleolar RENT complex. *Cell*. 97:233–244.

Shuster, C.B., and D.R. Burgess. 2002. Targeted new membrane addition in the cleavage furrow is a late, separate event in cytokinesis. *Proc. Natl. Acad. Sci. USA*. 99:3633–3638.

Sidrauski, C., and P. Walter. 1997. The transmembrane kinase Ire1p is a site-specific endonuclease that initiates mRNA splicing in the unfolded protein response. *Cell*. 90:1031–1039.

Skop, A.R., D. Bergmann, W.A. Mohler, and J.G. White. 2001. Completion of cytokinesis in C. elegans requires a brefeldin A-sensitive membrane accumulation at the cleavage furrow apex. *Curr. Biol.* 11:735–746.

Spear, E.D., and D.T. Ng. 2003. Stress tolerance of misfolded carboxypeptidase Y requires maintenance of protein trafficking and degradative pathways. *Mol. Biol. Cell*. 14:2756–2767.

Stegmeier, F., and A. Amon. 2004. Closing mitosis: the functions of the Cdc14 phosphatase and its regulation. *Annu. Rev. Genet*. 38:203–232.

Straight, A.F., W.F. Marshall, J.W. Sedat, and A.W. Murray. 1997. Mitosis in living budding yeast: anaphase A but no metaphase plate. *Science*. 277:574–578.

Swanson, R., M. Locher, and M. Hochstrasser. 2001. A conserved ubiquitin ligase of the nuclear envelope/endoplasmic reticulum that functions in both ER-associated and Matalpha2 repressor degradation. *Genes Dev.* 15:2660–2674.

Tolliday, N., L. VerPlank, and R. Li. 2002. Rho1 directs formin-mediated actin ring assembly during budding yeast cytokinesis. *Curr. Biol*. 12:1864–1870.

Travers, K.J., C.K. Patil, L. Wodicka, D.J. Lockhart, J.S. Weissman, and P. Walter. 2000. Functional and genomic analyses reveal an essential coordination between the unfolded protein response and ER-associated degradation. *Cell*. 101:249–258.

Tu, B.P., S.C. Ho-Schleyer, K.J. Travers, and J.S. Weissman. 2000. Biochemical basis of oxidative protein folding in the endoplasmic reticulum. *Science*. 290:1571–1574.

Vai, M., L. Popolo, and L. Alberghina. 1987. Effect of tunicamycin on cell cycle progression in budding yeast. *Exp. Cell Res.* 171:448–459.

Valdivia, R.H., and R. Schekman. 2003. The yeasts Rho1p and Pkc1p regulate the transport of chitin synthase III (Chs3p) from internal stores to the plasma membrane. *Proc. Natl. Acad. Sci. USA*. 100:10287–10292.

van Anken, E., E.P. Romijn, C. Maggioni, A. Mezghrani, R. Sitia, I. Braakman, and A.J. Heck. 2003. Sequential waves of functionally related proteins are expressed when B cells prepare for antibody secretion. *Immunity*. 18:243–253.

VerPlank, L., and R. Li. 2005. Cell cycle-regulated trafficking of Chs2 controls actomyosin ring stability during cytokinesis. *Mol. Biol. Cell*. 16:2529–2543.

Waddle, J.A., T.S. Karpova, R.H. Waterston, and J.A. Cooper. 1996. Movement of cortical actin patches in yeast. *J. Cell Biol.* 132:861–870.

Yeong, F.M. 2005. Severing all ties between mother and daughter: cell separation in budding yeast. *Mol. Microbiol.* 55:1325–1331.